Proceedings of ETCE2002
ASME Engineering Technology Conference on Energy
February 4-5, 2002, Houston, TX

ETCE2002/OT-29154

RHEOLOGICAL ANALYSIS OF CURING PROCESS OF EPOXY PREPREG USED AS COMPOSITE PIPE JOINTS

Liangfeng Sun and Arthur M. Sterling
Department of Chemical Engineering
Louisiana State University
Baton Rouge, Louisiana 70803

Su-Seng Pang
Department of Mechanical Engineering
Louisiana State University
Baton Rouge, Louisiana 70803

Michael A. Stubblefield
Center for Energy and Environmental Studies
Southern University
Baton Rouge, Louisiana 70813

ABSTRACT

The rheological properties of curing process of epoxy prepreg were measured by Bohlin Rheometer. The variations of storage modulus, loss modulus and viscosity are monitored vs. the cure time and temperature. Viscosity profiles were described by different models. Except the first order viscosity models, new viscosity models based on Boltzmann function were proposed. In the new models, a parameter called critical time was introduced. Critical time is a function of temperature and also meets an Arrhenius law. The activation energy calculated by critical time closes to that obtained by initial viscosity. The kinetic rate constants in the old and new models are comparable at each temperature, and the kinetic activation energies calculated from rate constants in the old and new models are very close. The fitting results show that the proposed new viscosity models are better than the old models for both isothermal and dynamic cure processes.

INTRODUCTION AND BACKGROUND

The domestic oil industry is vital to the American economy because of its dependence on hydrocarbons as a primary fuel source for industry and defense. However, domestic oil and gas reserves are declining. There are no more large land based reserves in the United States. A promising source for new oil and gas is from deep water (over 600 m) locations in the Gulf of Mexico. However, the cost of developing these deep water reserves is extremely expensive and the rate of return on investment, using current technology, does not justify the risk. The most economical deep water platform design is a Tension Leg Platform (TLP, see Fig. 1).

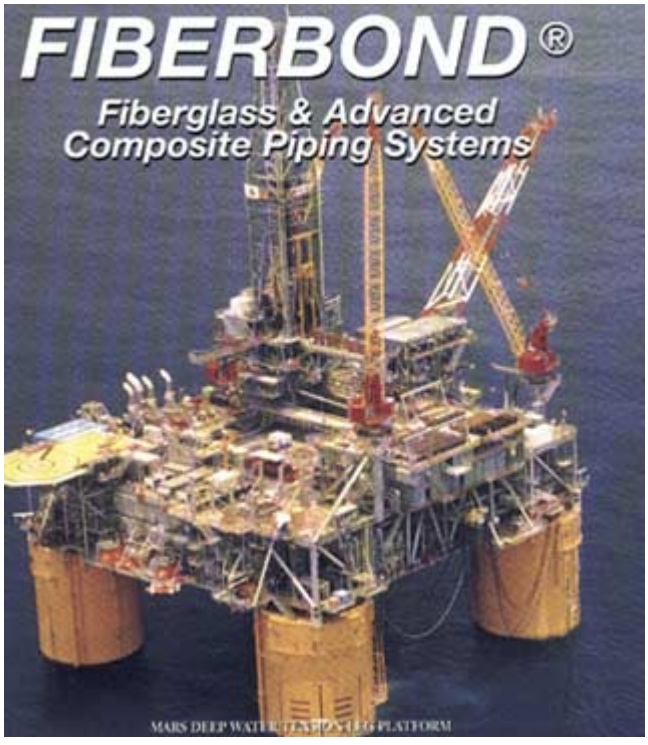

Fig. 1 Deep Water Tension Leg Platform

These TLPs are weight sensitive. It has been estimated that the use of advanced composites on the deck of the platform could greatly decrease the cost. A large percentage of the "dead weight" on the deck of a TLP is piping materials used for essential as well as non-essential services (see Fig. 2). Therefore, the weight of steel piping is an important factor in the high costs associated with the construction of deep water platforms.

Fig. 2 Pipe on the deck of a TLP

The acceptance of advanced composite pipe systems, utilizing reliable joining methods and lower cost fittings, will be a major contribution in the goal to obtain a 15-20% reduction in capital equipment costs required for domestic production equipment required to develop deep water reserves. Typical applications for advanced composite pipe systems on TLPs include service or process water, cooling medium, gray water (non hazardous waste), non hazardous drains, non hazardous vents, chemicals, firewater ringmain, firewater wet deluge, firewater dry deluge, produced water and ballast water. In order for the advanced composite pipe systems to receive acceptance, reliable joining methods and lower cost fittings must be developed to compete with heavy, often expensive, alloys in these applications. Piping systems on offshore platforms are considered "busy piping systems" due to the number of turns and bends in the piping arrangement. The benefits of composites - light weight, corrosion resistance, handling ease, etc., have long been appreciated, but the application has remained limited in the offshore oil and gas industry due to a lack of confidence in existing joint technology. A simple and cost effective promising approach for composite joining is by heat activated coupling. In this approach, the prepreg laminate is placed over the pipe joint. If heating is applied around the laminate, the thermoset resins will cure and laminate shrinks to seal the joints. An optimum cure cycle will help to improve the quality of the joints.

Applications of epoxy prepreg require understanding its rheological properties of the cure process, as well as the cure kinetics. Rheological analysis has been used to study the cure process of epoxy resin [1-4] and epoxy prepreg [5,6] and is essential to the optimization of cure cycle. Like polymers, epoxy prepreg is viscoelastic material. During curing process under continuous sinusoidal stresses or strains, its viscoelasticity experiences changes, which is reflected in the variations of rheological properties such as the storage modulus G', loss modulus G", viscosity η, and loss factor tan δ. The G' is the elastic character of the epoxy prepreg and reflects the energy that can be recoverable. The G" represents the viscous part of the epoxy prepreg and reflects loss energy by dissipation. Viscosity measures the fluidity of the epoxy resin system. Higher viscosity means the lower fluidity of the epoxy resin systems. The loss factor tan δ equals the ratio of the loss modulus to storage modulus. It is used to evaluate the viscoelasticity of the epoxy prepreg.

The flow behavior of reacting system is closely related to the cure process. In the early cure stage, the epoxy resin is in a liquid state. Cure reaction takes place in a continuous liquid phase. With the advancement of the cure process, crosslinking reaction occurs at a critical extent of reaction. This is the onset of formation of networking and called gel point [7]. At gel point, Epoxy resin changes from liquid to rubber state. It becomes very viscous and thus difficult to process; so the gelation has an important effect on the application process of epoxy prepreg. Although the appearance of the gelation limits greatly the fluidity of epoxy resins, it has little effect on the cure rate; so the gelation cannot be detected by the analysis of cure rate, as the case in the differential scanning calorimetry and Fourier transform infrared spectroscopy. The detection of gel time may be conducted by rheological analysis of cure process. The criteria to determine the gel time are to be discussed later.

Many rheological models have been developed to predict viscosity profiles of the cure process. The first order reaction viscosity models, to be discussed later, express viscosity as an exponential function of the cure time. Parameters in these models are easily determined by the rheological experimental data only. The first order reaction viscosity models have been frequently used in the rheological analysis of the cure process [8-12]. These models do not incorporate the effect of gelation on the viscosity and the predication accuracy is not good. The modified Williams-Landel-Ferry (WFL) models for viscosity [13-15] describe the variation of viscosity as a function of both cure temperature and glass transition temperature. These models have been extensively used. It was reported to achieve the good accuracy [15]. The applications of WFL models need to know the relationship between the glass transition temperature and cure time, which can be determined by thermal analysis. Percolation model for viscosity [16] express the variation of viscosity vs. degree of cure by power law. By introducing the degree of critical reaction into the model, the gel effect on the cure process was taken into account. It was reported that the percolation model fit the experimental data

quite well [16]. For the application of percolation model, kinetics law is necessary in order to determine the relationship of the degree of cure vs. time. The characteristics of other viscosity models for cure applications were discussed by Halley et al. [17].

This study is focused on the rheological properties of epoxy prepreg under isothermal and dynamic cure conditions. The first order reaction viscosity models are examined with experimental data. The new viscosity models are proposed and tested.

EXPERIMENTAL

Material

Commercial epoxy prepreg 8552 from Hexcel Corporation was used as samples for all the measurements.

Rheological Measurements

The isothermal and dynamic rheological measurements were conducted by Bohlin VOR Rheometer with parallel plates of 25 mm in diameter under the oscillation mode. The size of one layer of prepreg sample is 25.4 mm (1") in diameter and about 0.15 mm in thickness. Because one layer of epoxy prepreg is very thin, seven layers of the prepreg about 1 mm in thickness were used as the sample to improve measurements. Preliminary tests were conducted to determine the optimum instrumental parameters such as the angular frequency, gap between two plates, and strain. The optimized experimental conditions are the maximum strain of 0.18, a gap of about 1mm, and a frequency of 0.2 Hz. During experiments, the strain was set to be automatically adjustable to ensure the right torque range. For isothermal measurements, the sample chamber was preheated to the desired temperature and stabilized at that temperature for half hour. The sample was put into the chamber and measurement was start. For dynamic measurements, the samples were put into the chamber at the room temperature and heat at a certain rate.

RESULTS AND DISCUSSION

During the cure process, a sinusoidal strain or stress is applied to the sample and the response is monitored and recorded as storage modulus, loss modulus, viscosity, and phase angle in degree. A series of isothermal rheological measurements were carried out from 110 to 180 ^{o}C at 10 ^{o}C intervals, as well as dynamic rheological measurements. Fig. 3 shows the typical variations of storage modulus G' and loss modulus G" vs. time at 110 ^{o}C. During the initial cure period, the loss modulus is greater than storage modulus. The viscous character of the epoxy prepreg dominates its elasticity. In the final cure stage, the storage modulus is much greater than loss modulus. The epoxy prepreg becomes a mostly elastic solid. Under isothermal conditions, the storage modulus increases with the advancement of cure process, and finally reaches its plateau value while the loss modulus increases, reaches its maximum, and then decreases.

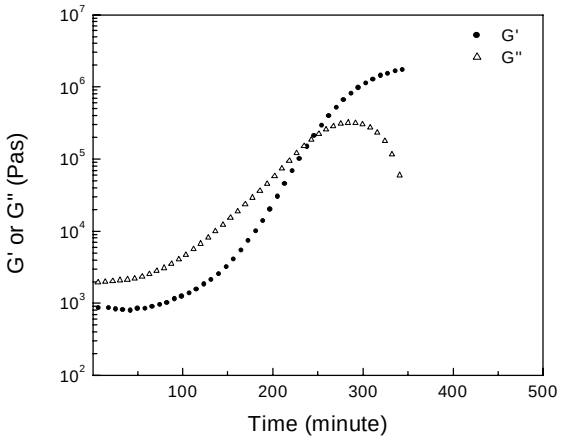

Fig. 3 Dependence of storage modules G' and loss modules G" on time at 110 ^{o}C

Rheological Modeling

During the curing process, the viscosity of the sample is not only the function of curing temperature, but also the function of degree of conversion. The viscosity change is the result of the combination of physical and chemical processes and can be empirically expressed as [11]:

$$\eta = \psi(T)\zeta(\alpha) \tag{1}$$

where $\psi(T)$ is a function of curing temperature only; $\zeta(\alpha)$ is a function of degree of conversion .

Terms $\psi(T)$ and $\zeta(\alpha)$ can be empirically expressed with the simple form respectively:

$$\psi(T) = \eta_0 \quad \text{and} \quad \zeta(\alpha) = \frac{1}{1-\alpha} \tag{2}$$

where η_0 is the initial viscosity; α is the degree of cure.

Substituting Eq. (2) into Eq. (1) to get Eq. (3),

$$\eta = \eta_0 \frac{1}{1-\alpha} \tag{3}$$

In Eq. (3), the initial viscosity η_0 depends on cure temperature and can be further expressed in Arrhenius equation,

$$\eta_0 = A_\eta e^{\frac{E_\eta}{RT}} \tag{4}$$

where A_η and E_η are the initial viscosity at $T = \infty$ and the viscous flow activation energy respectively.

The degree of cure α in Eq. (3) is a function of time. Depending on the cure kinetics, the relationship of α vs. time *t* may have different forms. For the first order reaction, it can be expressed as:

$$\frac{d\alpha}{dt} = k(1-\alpha) \tag{5}$$

and

$$k = A_k e^{-\frac{E_k}{RT}} \tag{6}$$

where A_k and E_k are the apparent rate constant at $T = \infty$ and the kinetic activation energy respectively.

Eq. (5) was solved to get Eq. (7),

$$\frac{1}{1-\alpha} = e^{\int_0^t k dt} \tag{7}$$

Substitute Eq. (7) into Eq. (3) to get:

$$\eta = \eta_0 e^{\int_0^t k dt} \tag{8}$$

or in the logarithmic form:

$$\ln \eta = \ln A_\eta + \frac{E_\eta}{RT} + A_k \int_0^t e^{-\frac{E_k}{RT}} dt \tag{9}$$

For the first order reaction with the isothermal cure process, temperature T and rate constant k are constant. Eqs. (8) and (9) become:

$$\eta = \eta_0 e^{kt} \tag{10}$$

$$\ln \eta = \ln A_\eta + \frac{E_\eta}{RT} + tA_k e^{-\frac{E_k}{RT}} \tag{11}$$

Eqs. (9) and (11) are the empirical four-parameter model of viscosity introduced by Roller [18]. According to Eq. (10), η_0 and k can be obtained from plot of $\ln\eta$ vs. t at each temperature. The values of A_η, E_η, A_k, and E_k are determined by Eqs. (4) and (6) respectively.

In the above models, the relationship of viscosity vs. time at isothermal conditions is a pure exponential type. These models are not accurate for the actual viscosity change. First, they fail to predict the occurrence of gel point, where the viscosity rises deeply. Secondly, the predicted final viscosity goes to infinity. So large error exists in the later cure stage.

Because of the limitation of the empirical models of viscosity, a new model of viscosity for isothermal cure process of epoxy resin systems is proposed:

$$\eta = \frac{\eta_0 - \eta_\infty}{1 + e^{k(t-t_c)}} + \eta_\infty \tag{12}$$

where η_0 and η_∞ are the initial and final viscosities respectively; k is the rate constant of cure reaction; and t_c is the critical time and obey an Arrhenius equation as a function of temperature,

$$t_c = A_t e^{\frac{E_t}{RT}} \tag{13}$$

Eq. (12) is proposed based on Boltzmann function to produce a sigmoidal curve, which viscosity profiles for the isothermal cure process follow. The parameters in Eq. (12) are determined by the multiple non-linear regression method.

For dynamic cure process, Eq. (12) becomes:

$$\eta = \frac{A_\eta e^{\frac{E_\eta}{RT}} - \eta_\infty}{1 + e^{\left(A_k \int_0^t e^{-\frac{E_k}{RT}} dt - A_k \int_0^{t_c} e^{-\frac{E_k}{RT}} dt\right)}} + \eta_\infty \tag{14}$$

The values of A_η and E_η are determined from the linear part of viscosity profile in the dynamic cure process. The determination of A_k and E_k is the same as previously discussed.

In the previous session, different viscosity models have been discussed. In this session, these models will be used to predict the isothermal viscosity change first. By Eq. (10), the initial viscosity η_0 and rate constant k are calculated respectively from the intercept and slope of the linear part of logarithmic viscosity vs. time before gel point. Their values at each isothermal temperature are listed in Table 1.

Table 1 Material parameters in Eqs. (11) and (9) at different isothermal cure temperatures

Temperature (°C)	ln(η_0) (pas)	Rate constant k (s^{-1})
110	6.1959 ± 0.0380	$3.739 \times 10^{-4} \pm 3.75 \times 10^{-6}$
120	5.8725 ± 0.0278	$5.900 \times 10^{-4} \pm 4.14 \times 10^{-6}$
130	5.0064 ± 0.0508	$9.306 \times 10^{-4} \pm 1.22 \times 10^{-5}$
140	4.8302 ± 0.0801	$1.57 \times 10^{-3} \pm 2.85 \times 10^{-5}$
150	4.2855 ± 0.1313	$2.60 \times 10^{-3} \pm 7.23 \times 10^{-5}$
160	4.0307 ± 0.0899	$4.44 \times 10^{-3} \pm 7.63 \times 10^{-5}$
170	3.1173 ± 0.2041	$6.99 \times 10^{-3} \pm 2.55 \times 10^{-4}$
180	3.2307 ± 0.0786	$1.061 \times 10^{-2} \pm 1.2 \times 10^{-4}$
Pre-exponential factor	$A_\eta = 2.0398 \times 10^{-6} \pm 1.4254 \times 10^{-6}$ Pas	$A_k = 9.916 \times 10^5 \pm 4.428 \times 10^5$ s^{-1}
Activation energy (J/mol)	$E_\eta = 6.2532 \times 10^4 \pm 2.992 \times 10^3$	$E_k = 6.9013 \times 10^4 \pm 1.661 \times 10^3$

As temperature increases, the initial viscosity decreases and the rate constant increases. Their relationship with temperature is given in Eqs. (4) and (6). The plots of logarithmic initial viscosity and rate constant vs. the reciprocal of temperature, including their linear fitting curves, are shown in Figs. 4 and 5 respectively. The values of A_η, E_η, A_k, and E_k

are determined from the linear fitting results and are also listed in Table 1.

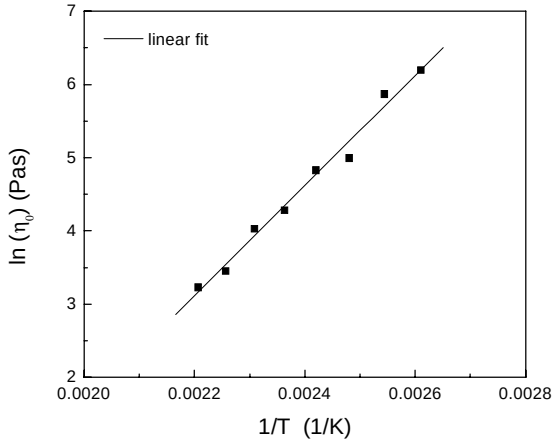

Fig. 4 Initial viscosity in Eq. (10) vs. isothermal cure temperature and the determination of the material parameters by Arrhenius equation

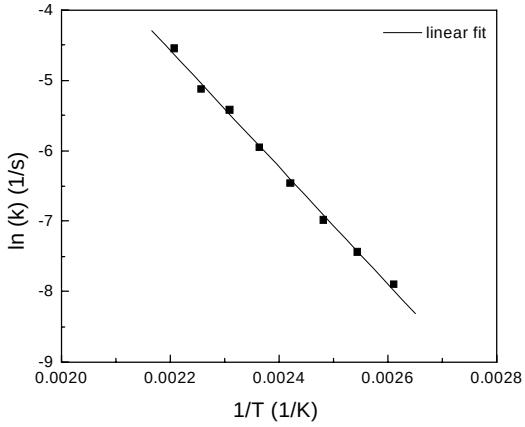

Fig. 5 Rate constant in Eq. (10) vs. cure temperature and the determination of the material parameters by Arrhenius equation

After determination of initial viscosity and rate constant at each temperature and parameters A_η, E_η, A_k, and E_k, the viscosity change at isothermal condition can be calculated by Eq. (10) or Eq. (11). The calculated viscosity by Eq. (10) and its comparison with experimental data are shown in Fig. 6. Large discrepancies occur in the region of gel point. This is attributed to the model that does not take into account of gel effect on the viscosity. As seen in Eq. (12), the proposed new viscosity model introduces two additional parameters, the critical time t_c and final viscosity η_∞. All the parameters η_0, η_∞, t_c and k in Eq. (12) are determined at the same time by fitting experimental viscosity with respect to time by nonlinear least square approach. The fitting results are also shown in Fig. 6. The predicted viscosities have very good agreement with the experimental data, even in the gel region. It seems clearly that the viscosity change can be described by the proposed new viscosity model. The values of critical time and rate constant at each temperature are listed in Table 2.

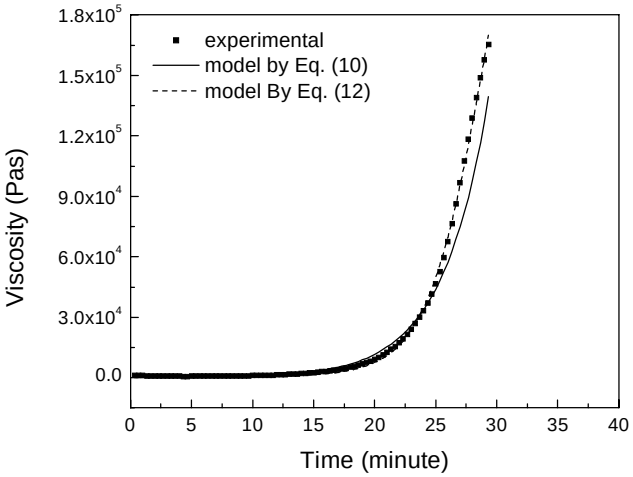

Fig. 6 Experimental and calculated viscosity profiles at 160 ^{o}C

Table 2 Material parameters in Eqs. (12) and (13) at different isothermal cure temperatures

Temperature (^{o}C)	Critical time t_c (s)	Rate constant k (s^{-1})
110	15519.5 ± 49.5	6.052 x 10^{-4} ± 4.29 x 10^{-6}
120	10024.2 ± 26.0	9.554 x 10^{-4} ± 1.02 x 10^{-5}
130	6710.5 ± 30.6	1.734 x 10^{-3} ± 3.41 x 10^{-5}
140	4107.2 ± 14.7	2.888 x 10^{-3} ± 6.00 x 10^{-5}
150	2594.1 ± 11.1	4.623 x 10^{-3} ± 8.72 x 10^{-5}
160	1742.0 ± 11.8	7.045 x 10^{-3} ± 1.27 x 10^{-4}
170	1133.2 ± 3.3	1.257 x 10^{-2} ± 1.4 x 10^{-4}
180	783.7 ± 5.7	1.372 x 10^{-2} ± 3.7 x 10^{-4}
Pre-exponential factor (s^{-1})	A_t = 5.3887 x 10^{-5} ± 1.45 x 10^{-7}	A_k=1.3157 x 10^6 ± 7.395 x 10^5
Activation energy (J/mol)	E_t = 6.2337 x 10^4 ± 9.57 x 10^2	E_k=6.7887 x 10^4 ± 2.200 x 10^3

The variations in critical time with respect to temperature can also be described by an Arrhenius equation. As seen in Fig. 7, there is a very linear relationship between the logarithmic critical time and the reciprocal of absolute temperature. The rate constant in Eq. (12) is larger than that in Eq. (10) for the same temperature and also obeys an Arrhenius equation as a function of temperature. The relationship of $\ln k$ vs. $1/T$ and the linear fitting curve are given in Fig. 8. The fitting values of pre-exponential factors and activation energies are listed in Table 2. The kinetic activation energy obtained from rate constant in Eq. (12) is 67.9 KJ/mol, which is closed to the value of 69 KJ/mol obtained from rate constant in Eq. (10). It is also interesting to note that the activation energies obtained from initial viscosity in Eq. (4), and critical time in Eq. (13) are closed each other, with the values of 62.5, and 62.3 KJ/mol, respectively.

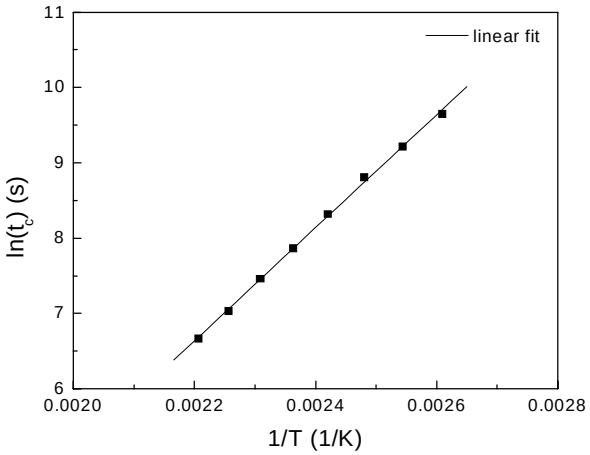

Fig. 7 Critical time in Eq. (12) vs. cure temperature

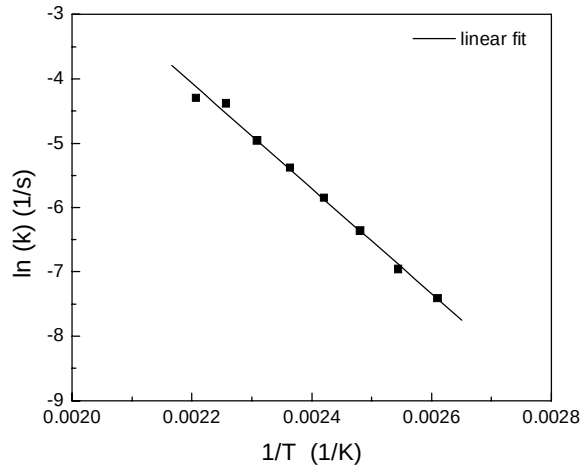

Fig. 8 Rate constant in Eq. (12) vs. isothermal cure temperature and the determination of the material parameters by Arrhenius equation

The model parameters obtained from isothermal conditionals are useful to the study of variation of dynamic viscosities with respect to temperature. Fig. 9 gives the logarithmic plots of dynamic viscosity vs. temperature at heating rates of 2 and 5 $^{o}C/min$.

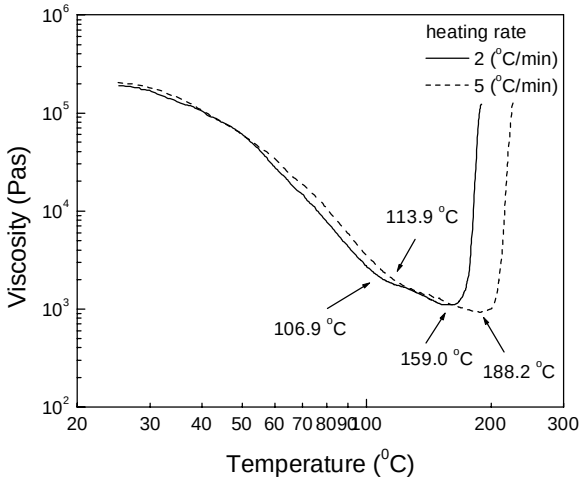

Fig. 9 Logarithmic plot of viscosity vs. temperature at heating rates of 2 and 5 ^{o}C/min

At each heating rate, the curve shows the onset temperature of cure reaction and the minimum viscosity temperature. As heating rate increases, the onset temperature of cure reaction increases from 106.9 to 113.9 ^{o}C, and the minimum viscosity temperature increases from 159 to 188.2 ^{o}C. The values of onset temperature of cure reaction at heating rates of 2 and 5 $^{o}C/min$ are closed to those obtained by DSC measurements, which occur at 110 and 114.5 ^{o}C respectively. It is also worth noting that the minimum viscosity decreases with the increment of heating rate. As it reaches to the minimum viscosity, the epoxy resin system has the greatest flow ability. But the cure reaction rate does not necessarily achieve the fastest at the minimum temperature because the DSC kinetic study showed that the cure process was kinetically controlled. The minimum viscosity has an important effect on the application of epoxy prepreg. If the minimum viscosity is too low, it may cause the epoxy resin to distribute unevenly among reinforced fibers.

The variation of viscosity during dynamic cure process can be described by dynamic models previously discussed, as seen in Eqs. (9) and (14). The kinetic parameters A_k and E_k in the dynamic models have been determined from isothermal rate constants. To improve the fitting results, the viscous flow parameters A_η and E_η in the dynamic models were determined by fitting the linear part of the plot of viscosity vs. time before cure reaction under dynamic conditions. The calculated values for A_η and E_η were 8.20×10^{-5} Pas and 54.7 KJ/mol, respectively.

The viscous flow activation energy determined from dynamic cure process is lower than that determined from isothermal conditions. The terms with integrating parts in the dynamic models were determined by software using the trapezoidal rule. The critical time t_c in Eq. (14) were determined by a nonlinear least square regression method. The viscosities calculated by Eqs. (9) and (14) and the comparison with experimental data at heating rates of 2 and 5 ^{o}C/min are shown in Figs. 10 and 11 respectively. It is clear the new model based on Boltzmann function is better than the first order reaction dynamic model.

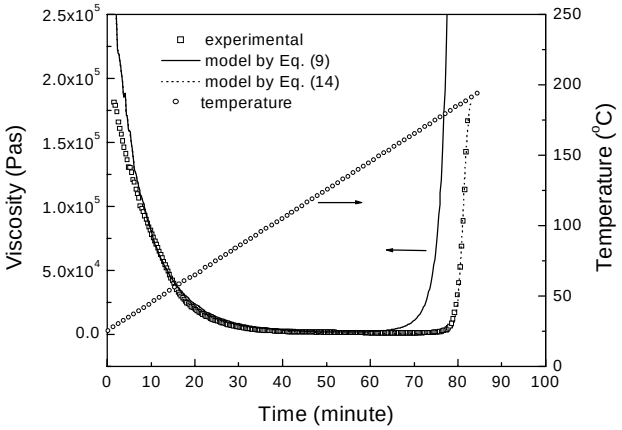

Fig. 10 The Experimental and calculated dynamic viscosity at a heating rate of 2 ^{o}C/min; The critical time t_c in Eq. (14) is 81.2 *minutes* and the corresponding critical temperature is 187.4 ^{o}C

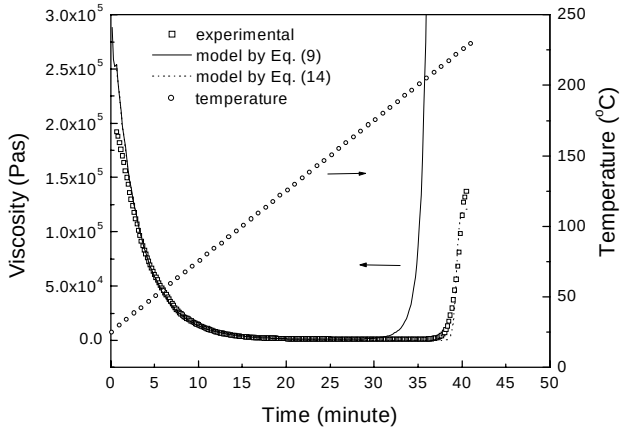

Fig. 11 The Experimental and calculated dynamic viscosity profiles at a heating rate of 5 ^{o}C/min. The critical time t_c in Eq. (14) is 39.4 *minutes* and the corresponding critical temperature is 221.8 ^{o}C

CONCLUSIONS

Rheological analysis is required in order to optimize the curing process. Rheological properties such as storage modulus, loss modulus, and viscosity are closely related to the cure temperature and time. During the curing process, the variation of viscosity vs. time is predictable by several viscosity models. Under isothermal conditions, the empirical first order reaction viscosity model has a larger deviation from the experimental data. The proposed new viscosity based on the Boltzmann function agrees very well with the experimental data. The critical time in the new model decreases with the increment of the isothermal temperature and their relationship can be described by Arrhenius equation. The activation energies determined by initial viscosity, and critical time are close each other. At the same temperatures, the kinetic rate constants in the first reaction viscosity model are in the same ranges as those in the new viscosity model. The calculated kinetic activation energies are very close. For the dynamic curing process, the empirical viscosity model is less superior than the new model. The proposed new viscosity model improves the fitting results. As the heating rate increases, the minimum viscosity decreases and the temperature corresponding to the minimum viscosity increases. At the temperature corresponding to minimum viscosity, the cure rate is not necessarily the fastest.

ACKNOWLEDGMENTS

This investigation was partially sponsored by NASA/FAR program under contract number NAG8-1536 as well as the Louisiana Board of Regents under contract numbers LEQSF (1998-01)-RD-A-27, LEQSF (2000-03)-RD-B-05 and LEQSF (2001-04)-RD-B-03.

REFERENCES

1. W. V. Breitigam, R. S. Bauer, and C. May, *Polymer*, **34**, 767 (1993)
2. A. B. Spoelstra, G. W. M. Peters, and H. E. H. Meijer, *Polym. Eng. Sci.*, **36,** 2153 (1996).
3. A. Ya. Malkin and S. G. Kulichikhin, *Polym. Eng. Sci.*, **37,** 1322 (1997).
4. D. S. Kim, *J. Appl. Polym. Sci.*, **80**, 873 (2001).
5. M. R. Dusi, R. M. Galeos, and M. G. Maximovich, *J. Appl. Polym. Sci.*, **30**, 1847 (1985).
6. B. S. Hayes, E. N. Gilbert, and J. C. Seferis, *Composites*, Part A, 31, 717 (2000).
7. C.-Y. M. Tung and P. J. Dynes, *J. Appl. Polym. Sci.*, **27**, 569 (1982).
8. J. M. Barton, D. C. L. Greenfield, and K. A. Hodd, *Polymer*, **33**, 1177 (1992).
9. Q. Wang, T. He, P. Xia, T. Chen, and B. Huang, *J. Appl. Polym. Sci.*, **66**, 799 (1997).
10. R. P. Theriault, T. A. Osswald, andJ. M. Castro, *Polym. Compos.*, **20**, 628 (1999).

11. J. Ampudia, E. Larrauri, E. M. Gil, M. Rodriguez, and L. M. Leon, *J. Appl. Polym. Sci.*, **71**, 1239 (1997).
12. M. R. Dusi, C. A. may, and J. C. Seferis, *ACS Symp. Ser.*, **227**, 301 (1983).
13. Y. A. Tajima and D. Crozier, *Polym. Eng. Sci.*, **23,** 186 (1983).
14. J. Mijovic and C. Hung Lee, *J. Appl. Polym. Sci.*, **37**, 889 (1989).
15. P. I. Karkanas and I. K. Partrige, *J. Appl. Polym. Sci.*, **77**, 2178 (2000).
16. D. Serrano, J. Peyrelasse, C. Boned, D. Harran, and P. M.onge, *J. Appl. Polym. Sci.*, **39**, 679 (1990).
17. P. J. Halley and M. E. Mackay, *Polym. Eng. Sci.*, **36,** 593 (1996).
18. M. B. Roller, *Polym. Eng. Sci.*, **15,** 406 (1975).